



Morphological prediction of lethal outcomes in the evaluation of lung tissue structural changes in patients on respiratory support with COVID-19: Ukrainian experience

Viktoriya Matskevych^a, Olexandr Kamyshnyi^b, Volodymyr M. Vasylyk^c, Marta B. Grynovska^d, Tetiana Lenchuk^a, Roman Fishchuk^e, Dmytro Gospodaryov^f, Ihor Yurkevych^f, Olha Strilbytska^f, Pavlo Petakh^{b,g,*}, Oleh Lushchak^{f,h,**}

^a Department of Radiology and Radiation Medicine, Ivano-Frankivsk National Medical University, Ukraine

^b Department of Microbiology, Virology and Immunology, I. Horbachevsky Ternopil National Medical University, Ternopil, Ukraine

^c Pathology Department, Municipal Non-profit Enterprise "Regional Clinical Hospital of Ivano-Frankivsk Regional Council", Ivano-Frankivsk, Ukraine

^d Department of Anesthesiology and Intensive Care, Ivano-Frankivsk National Medical University, Ukraine

^e Clinical Trials Unit, Municipal Non-profit Enterprise "Ivano-Frankivsk Central City Hospital", Ukraine

^f Department of Biochemistry and Biotechnology, Vasyl Stefanyk Precarpathian National University, Ivano-Frankivsk, Ukraine

^g Department of Biochemistry and Pharmacology, Uzhhorod National University, Uzhhorod, Ukraine

^h Research and Development University, Ivano-Frankivsk, Ukraine

ARTICLE INFO

Keywords:

Coronavirus infection
SARS-CoV-2
Diffuse alveolar damage
Autopsy
Ground glass opacity

ABSTRACT

The impact of the severe acute respiratory syndrome coronavirus 2 (SARS-CoV-2) on lung tissue in patients on respiratory support is of significant scientific interest in predicting mortality. This study aimed to analyze post-mortem histological changes in the lung tissue of COVID-19 patients on respiratory support using vital radiology semiotics. A total of 41 autopsies were performed on patients who died of SARS-CoV-2 and had confirmed COVID-19 by polymerase chain reaction (PCR) and radiological evidence of lung tissue consolidation and ground glass opacity. The results showed that the duration of COVID-19 in patients on respiratory support was significantly associated with the development of all stages of diffuse alveolar damage, acute fibrous organizing pneumonia, pulmonary capillary congestion, fibrin thrombi, perivascular inflammation, alveolar hemorrhage, proliferating interstitial fibroblasts, and pulmonary embolism. The prediction model for lethal outcomes based on the duration of total respiratory support had a sensitivity of 68.3% and a specificity of 87.5%. In conclusion, for COVID-19 patients on long-term respiratory support with radiological signs of ground glass opacity and lung consolidation, post-mortem morphological features included various stages of diffuse alveolar lung damage, pulmonary capillary congestion, fibrin clots, and perivascular inflammation.

1. Introduction

According to the World Health Organization (WHO), 762 791 152, cases of coronavirus infection (COVID-19) have been reported worldwide, of which 6 897 025 ones were fatal. About 5 484 936 cases of this disease were reported in Ukraine with 111 789 outcomes (as of April 12, 2023) [1]. It is known about the multitarget damage of various organs and systems by COVID-19 and the main target for Severe Acute Respiratory Syndrome Coronavirus 2 (SARS-CoV-2) are alveolar epitheliocytes of the lungs, where the binding of viral S-protein with

angiotensin-converting enzyme 2 can occur for virus replication with subsequent development of a cascade of pathophysiological responses and leads to the activation of humoral and cellular immunity [2]. Development of hypoxemic respiratory failure in patients with severe disease is characterized by respiratory rate ≥ 30 / min, oxygen saturation $\leq 93\%$, ratio of arterial oxygen partial pressure to fractional inspired oxygen (PaO₂ / FiO₂ ratio) < 300 mm Hg or pulmonary infiltrates taking up more than 50% of pulmonary fields. The above-mentioned conditions require immediate initiation of oxygen therapy with nasal cannulas or devices with high-flow oxygen delivery

* Corresponding author at: Department of Microbiology, Virology and Immunology, I. Horbachevsky Ternopil National Medical University, Ternopil, Ukraine.

** Corresponding author at: Department of Biochemistry and Biotechnology, Vasyl Stefanyk Precarpathian National University, Ivano-Frankivsk, Ukraine.

E-mail addresses: pavlo.petakh@uzhnu.edu.ua (P. Petakh), oleh.lushchak@pnu.edu.ua (O. Lushchak).

<https://doi.org/10.1016/j.prp.2023.154471>

Received 10 February 2023; Received in revised form 18 April 2023; Accepted 18 April 2023

Available online 23 April 2023

0344-0338/© 2023 The Author(s).

Published by Elsevier GmbH. This is an open access article under the CC BY license

(<http://creativecommons.org/licenses/by/4.0/>).

[3]. It should be noted that dyspnea and the proportionality of patient's condition to laboratory and radiological parameters are not always characteristic of respiratory failure in coronavirus infection, which often causes delayed medical treatment and high mortality [4]. Risk factors for acute respiratory failure include male gender, age over 60 years, and comorbidities such as diabetes, malignancies and immunodeficiency [5]. The range of histopathological findings in patients who have died of COVID-19 is very various, ranging from the predominance of diffuse alveolar lung damage according to some studies, ending with a discussion of the phenotype of pulmonary acute respiratory distress syndrome [6]. It should also be noted that it remains to be seen which of the pathomorphological lungs features of deceased patients who were on artificial respiratory support are caused by the disease itself, and which are secondary due to prolonged invasive ventilation [7]. Therefore, due to the high scientific interest in the mechanisms of pathological complications of COVID-19 and the challenges faced by the health care system, studies with the possibility of establishing correlations between duration, type of respiratory support and morphological changes in lung tissue remain relevant and, consequently, the prediction of lethal consequences in accordance with the obtained results are valuable. Therefore, the aim of our study was analysis of postmortal histological changes in the lung tissue of patients on respiratory support with vital appropriate radiology lung semiotics, who died of COVID-19.

2. Materials and methods

2.1. Study groups

We conducted a prospective cohort study of patients who were hospitalized in the period from October 2020 to July 2021. COVID-19 was diagnosed for 41 patients antemortem by polymerase chain reaction (PCR) of nasopharyngeal smear, which was confirmed also in postmortem samples by the same laboratory method of sectional material, which was the main criterion for inclusion in the study group. Diagnostics for disease was carried out in laboratories accredited by the

Ministry of Health of Ukraine, which can conduct testing for COVID-19 by the PCR method. Verification of the research methodology is carried out by the laboratory of the State Institution "Public Health Center of the Ministry of Health of Ukraine" or regional laboratory centers of the Ministry of Health of Ukraine.

The basis for data processing is the written informational consent of the legally authorized person of the deceased patient to process the received data on the basis of confidential processing. The exclusion criteria were: 1) age up to 18 years; 2) chronic comorbidities of the bronchopulmonary system (tuberculosis, bronchial asthma, fibrosing alveolitis); 3) human immunodeficiency virus and Acquired Immune Deficiency Syndrome; 4) patients who have previously used oxygen concentrators at home. The control group included the results of 32 deceased patients without respiratory pathology, but who received invasive mechanical ventilation in coma of various etiologies, such as: renal, cardiac, cerebral, hepatic failure, ketoacidotic coma and others; patients during surgery and in the postoperative period. Patients were excluded from the study due to personal decision of the legally authorized person of the deceased person. More detailed information on the characteristics of the control and experimental groups is presented in the [supplementary table 1](#) (Suppl. Table 1). The diagnostic examination complied with according to the guidelines of the Declaration of Helsinki, and approved by the Ethics Committee of Ivano-Frankivsk National Medical University (Protocol No 116/20 of 07.10.2020).

2.2. Macro- and microscopic examination of lungs

The post-mortem study was conducted in compliance with the measures of biological safety of personnel working with biological material of the deceased in a complete and equipped quarantine autopsy room for particularly dangerous infectious diseases. Collection of material for the study was performed in triplicate, including the mucosa of the upper and lower respiratory tract, the most affected areas of lung tissue to determine the location of virus replication and microscopic studies. Samples for morphological examination were immersed in

Table 1
Morphological signs of lungs of patients belonged to the control group and group with COVID-19.

Histology signs	Categories	Control group	Study group	p	
Histological diagnosis	Normal	31 (42.5)	0 (0.0)	< 0.001 *	
	Diffuse alveolar damage (DAD)	2 (2.7)	36 (49.3)	$p_{\text{normal}} - \text{DAD} < 0.001$	
	Acute fibrous organizing pneumonia (AFOP)	0 (0.0)	4 (5.5)	$p_{\text{normal}} - \text{AFOP} < 0.001$	
Pulmonary embolism	Absent	28 (38.4)	15 (20.5)	< 0.001 *	
	Present	5 (6.8)	25 (34.2)		
Hyaline Membranes	Absent	Rare	30 (41.1)	< 0.001 *	
		Rare	1 (1.4)	$p_{\text{absent}} - \text{rare} < 0.001$	
		Focal	0 (0.0)	22 (300.1)	$p_{\text{absent}} - \text{focal} < 0.001$
		Diffuse	2 (2.7)	13 (17.8)	$p_{\text{absent}} - \text{diffuse} < 0.001$
Pulmonary capillary congestion	Absent	29 (39.7)	3 (4.1)	< 0.001 *	
		Present	4 (5.5)	37 (50.7)	
Fibrin thrombi	Absent	27 (37.0)	13 (17.8)		
		Rare	5 (6.8)	21 (288)	< 0.001 *
		Focal	0 (0.0)	6(8.2)	$p_{\text{absent}} - \text{rare} < 0.001$
		Diffuse	1 (1.4)	0 (0.0)	$p_{\text{absent}} - \text{focal} = 0.035$
Intra-alveolar fibrin organization	Absent	33 (45.2)	23 (31.5)	< 0.001 *	
		Rare	0 (0.0)	14 (19.2)	$p_{\text{absent}} - \text{rare} = 0.002$
		Diffuse	0 (0.0)	3 (4.1)	
Lymphocytic alveolitis	Absent	30 (41.1)	19 (26.0)	< 0.001 *	
		Present	3 (4.1)	21 (28.8)	
Perivascular inflammation	Absent	31 (42.5)	9 (12.3)	< 0.001 *	
		Present	2 (2.7)	31 (42.5)	
Fibrinoid necrosis of vascular walls	Absent	31 (42.5)	25 (34.2)	0.009 *	
		Present	2 (2.7)	15 (20.5)	
Alveolar hemorrhages	Absent	28 (38.4)	11 (15.1)	< 0.001 *	
		Rare	5 (6.8)	23 (31.8)	$p_{\text{absent}} - \text{rare} < 0.001$
		Diffuse	0 (0.0)	6 (8.2)	$p_{\text{absent}} - \text{diffuse} < 0.001$
Proliferating interstitial fibroblasts	Absent	30 (41.1)	18 (24.7)	< 0.001 *	
		Rare	3 (4.1)	20 (27.4)	$p_{\text{absent}} - \text{focal} < 0.001$
		Diffuse	0 (0.0)	2 (2.7)	

neutral 10% formalin for fixation [8]. Formalin-fixed morphological tissues were embedded in paraffin in 72 h, [9]. Sections of paraffin blocks (thickness of 4 μm) were obtained on a sledge microtome, followed by hematoxylin-eosin staining.

2.3. Statistical analysis

Statistica 12 software was used for statistical analysis. The Shapiro-Wilk test (less than 50) or the Kolmogorov-Smirnov test (more than 50) were used for quantitative normal data. The median (Me) and lower and upper quartiles (Q1 - Q3) were used for assessment of non-normal distribution. Categorical data were described with absolute values and percentages. The comparison of the two groups on a quantitative indicator, the distribution of which differed from normal, was performed using the Mann-Whitney U-test. Comparisons of three or more groups on a quantitative indicator, the distribution of which differed from normal, were performed using the Kruskal-Wallis test, a posteriori comparisons - using the Dunn test with the Hill correction. Comparison of percentages in the analysis of four-pole correlation tables was performed using Pearson's chi-square test (for expected values greater than 10), Fisher's exact test (for expected values less than 10). Comparison of percentages in the analysis of multifield conjugation tables was performed using the Pearson chi-square test. Correlations were conducted using Kendall rank correlation, as presented in Fig. 1. Principal component analysis was performed using R packages 'base'. Parameters of receiver operating characteristics (ROC) curves were visualized using R package 'pROC'. All plots were drawn, using R package 'ggplot2'.

3. Results

The diagnosis of COVID-19 determined by different methods did not

significantly correlate with age of all patients as well as with gender (Fig. 1A). However, there were significant inverse correlations between radiology signs, characteristic of COVID-19, and such causes of death as acute embolism and thrombosis of unspecified deep veins of lower extremity, acute cerebral infarction, acute vascular disorders of intestine, acute haemorrhagic stroke, acute peptic/duodenal ulcer with both hemorrhage and perforation.

Indeed, the control and COVID-19 groups were uniform by gender, containing about 63% of males and about 47% females (Fig. 2). They contained relatively small percentages of patients with diagnosed urolithiasis, psoriasis, obesity, postinfarction cardiosclerosis, cerebrovascular and kidney diseases (Fig. 2). However, control group contained significantly higher number of patients with diagnosed anemia, peptic ulcer disease, and thrombosis of unspecified deep veins of distal lower extremity, whereas COVID-19 group contained a larger number of patients with diabetes (Fig. 2). Both groups comprised similar but relatively high percent (50–60%) of the individuals with obliterative atherosclerosis, heart failure, coronary artery disease, and hypertension. There was also no difference in age between patients (Fig. 3A).

Both study and comparison groups comprised patients who were without respiratory support and patients whose breathing was supported by supplemental oxygen. Five patients from the study group did not receive oxygen support because they did not have respiratory failure and died from thromboembolism, acute myocardial infarction and stroke due to coronavirus infection. Thirty six patients received oxygen therapy with facial mask, continuous positive airway pressure therapy, mechanical invasive ventilation with intubation. The average length of hospital stay for the study group was 16 days (the shortest period was 1 day and the longest was 83 days, respectively). The average length of hospital stay for the control group was 8 days (range of hospitalization period was 1 – 47 days, respectively). The average duration of oxygen

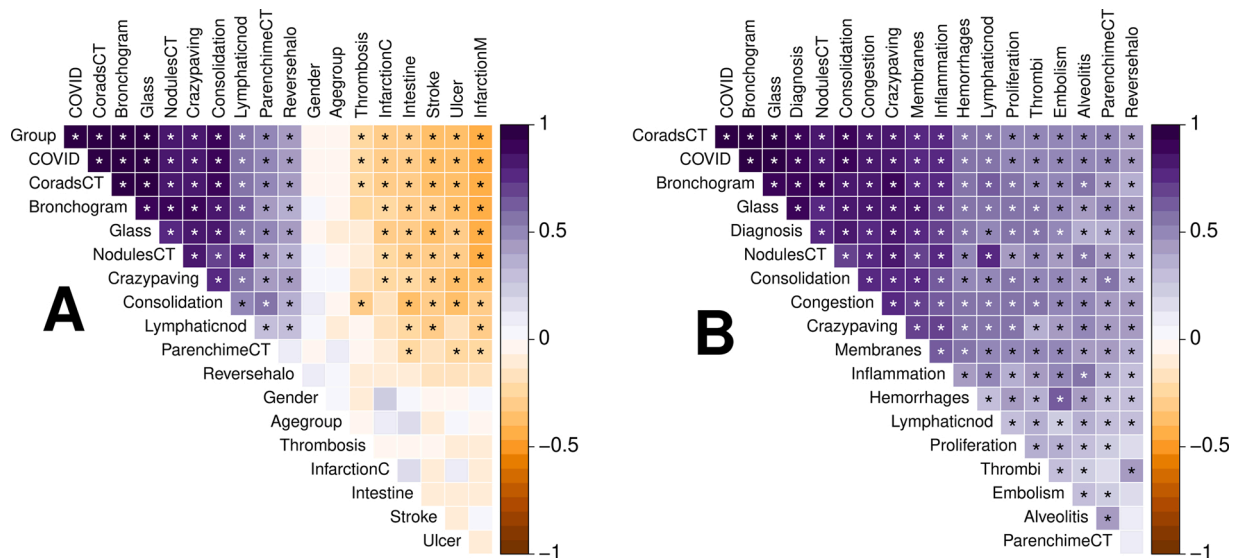


Fig. 1. Kendall rank correlation matrices between A) radiology signs and characteristics of individuals belonging to groups studied, and B) radiology signs and histological signs of individuals studied. Asterisk denotes significant (p < 0.05) correlations. "Group" denotes individuals of the control group and individuals died with diagnosis of COVID-19, "COVID-19" – the same as previous but groups were assigned on the basis of PCR and/or immunological testing (International Classification of Diseases 10 (ICD-10), code U07.1), "CoradsCT" – control and COVID-19 groups were assigned according to the COVID-19 Reporting and Data System (CO-RADS) and basing on radiology signs (computer tomography – CT); control individuals were of category 1, whereas individuals of investigation group had category 5 (typical COVID-19), "Bronchogram" – air bronchogram sign, "Glass" – ground glass opacity (basing on either CT or X-ray imaging), "NodulesCT" – enlarged mediastinal lymphatic nodules (CT), "Crazy paving" – crazy-paving pattern (CT), "Consolidation" – lung consolidation (CT and ultrasonography), "Lymphaticnod" – lower paratracheal lymphatic nodules' size in cm (short axis of the maximal large nodule) (CT), "ParenchimeCT" – involving lung parenchime percentage (%) (CT), "Reversehalo" – reversed halo sign (CT), "Thrombosis" – acute embolism and thrombosis of unspecified deep veins of lower extremity (ICD-10 code I82.4), "InfarctionC" – acute cerebral infarction (ICD-10 code I61), "Intestine" – acute vascular disorders of intestine (ICD-10 code K55.0), "Stroke" – acute haemorrhagic stroke (ICD-10 code I63), "Ulcer" – acute peptic /duodenal ulcer with both hemorrhage and perforation (ICD-10 codes K26.2/K27.2), "Diagnosis" – histological diagnosis, "Congestion" – pulmonary capillary congestion, "Membranes" – hyaline membranes, "Inflammation" – perivascular inflammation, "Hemorrhages" – alveolar hemorrhages, "Proliferation" – proliferating interstitial fibroblasts, "Thrombi" – fibrin thrombi, "Embolism" – pulmonary embolism, "Alveolitis" – lymphocytic alveolitis.

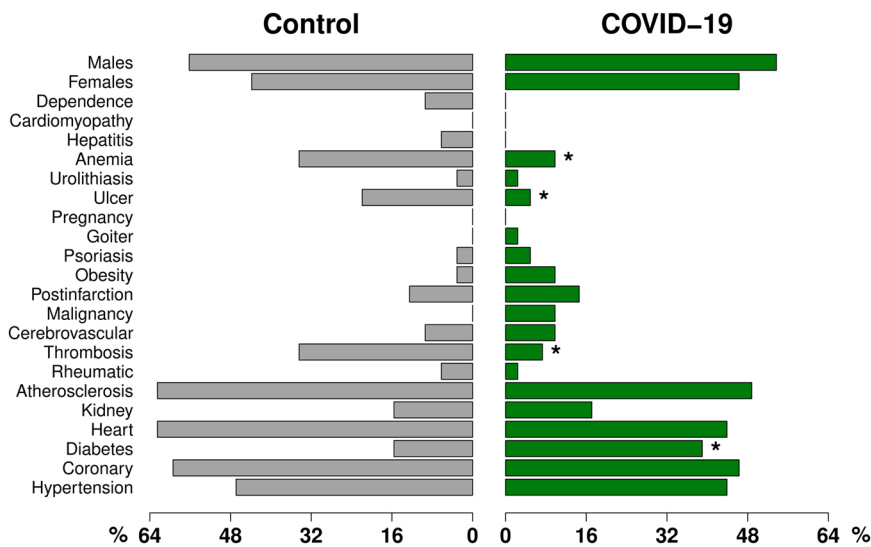


Fig. 2. Percent comorbidities and other characteristics of the control and study group. Asterisks denote significant difference evaluated by Fisher’s exact test ($p < 0.05$). Unless where it is obvious, abbreviations are as follows: “Dependence” – alcohol dependence, “Hepatitis” – chronic viral hepatitis, “Ulcer” – peptic ulcer disease in anamnesis, “Goiter” – nontoxic multinodular goiter, “Postinfarction” – postinfarction cardiosclerosis (syn. – old myocardial infarction), “Cerebrovascular” – cerebrovascular diseases in anamnesis, “Thrombosis” – thrombosis of unspecified deep veins of distal lower extremity, bilateral, “Rheumatic” – rheumatism, rheumatic diseases of endocardium, valve, “Atherosclerosis” – obliterative atherosclerosis, “Kidney” – chronic kidney diseases, “Heart” – heart failure, “Diabetes” – diabetes mellitus; “Coronary” – coronary artery disease.

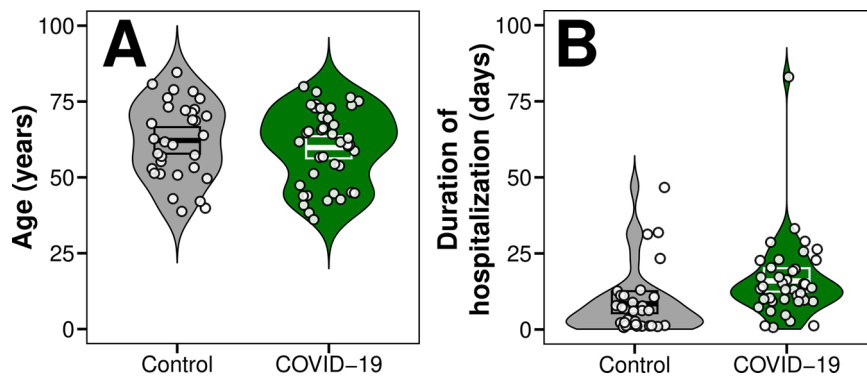


Fig. 3. Violin plots that show (A) age distribution of the control and study groups, and (B) distribution of the control and study group by duration of hospitalization. The boxes show mean (midline) and lower and upper confidence levels (floor and ceiling of the boxes).

support for the study group was 11 days (range of respiratory support was 1–78 days, respectively). The average duration of oxygen support for the control group was 8 days (range of respiratory support was 1–11 days, respectively) (Fig. 4). All patients underwent in vivo radiological examinations, often in dynamics, which, according to the doctor’s prescription, included ultrasound diagnosis of the lungs, X-ray and computed tomography of the lungs, combinations, and frequency of which were prescribed according to the clinical needs of each individual

case (Fig. 4, Suppl. Table 1).

During radiology examination (assessment at the stage of worsening when saturation had decreased) lung consolidation with crazy-paving pattern and patchy ground-glass opacities was detected: both lungs in 37 patients (90%) and unilaterally in 4 patients (10%). The consolidation areas were peripherally placed. Reverse halo sign was observed in 14 patients (34%). Lung parenchyma involving was as follows: 13 patients (32%) had 25–30%, 9 patients (22%) had 35–50%, 14 patients



Fig. 4. Chest X-ray images in the dynamics of patient K., 62 years old with confirmed COVID-19, concomitant diabetes mellitus and coronary heart disease. A. At admission - bilateral consolidation with areas of ground glass, located peripherally. B - pronounced negative dynamics after 2 days: areas of consolidation and ground glass occupy both pulmonary fields, the heart is dilated in diameter (additional signs of myocardial damage at subsequent autopsy).

(34%) had 55–75% and 5 patients (12%) had over 80% parenchyma injury. The walls of the bronchi were mild thickened in all patients. Mediastinal lymph nodes were enlarged to 1.1–1.5 cm in short axis in 37 patients (90%). Radiology signs of all COVID-19 patients corresponded to CO-RADS 5 level (COVID-19 Reporting and Data System developed by the Dutch Radiological Society) (Fig. 5).

In 33 patients, coronavirus infection was detected in vivo by PCR from nasopharyngeal lavage, and in 8 patients - established postmortem also by PCR of selected pieces of trachea, bronchi and lung tissue. The autopsies were performed on the same or next day but not more than 16 h after the death.

There were such histological findings in patients with COVID-19 disease (who received in the hospital oxygen therapy) as: development of diffuse alveolar damage (DAD) in different stages at the moment of autopsy, acute fibrosing organizing pneumonia (AFOP) signs, pulmonary capillary congestion, fibrin thrombi, alveolar hemorrhage, proliferating interstitial fibroblasts, intraalveolar fibrin organization, the appearance of single, uniform and heterogeneous alveolitis (Fig. 6). There were also such common peculiarities as perivascular inflammation, fibrinoid vessel wall necrosis, pulmonary embolism in the majority of study cases.

There was no significant difference observed between the duration and the occurrence of fibrinoid necrosis of vascular walls in the study and control groups ($p = 0.610$; Fig. 7J). Lymphocytic alveolitis ($p = 0.010$), perivascular inflammation ($p = 0.017$), hemorrhage ($p = 0.020$), pulmonary embolism ($p = 0.011$) were also found in patients treated with oxygen therapy from the beginning of hospitalization (Fig. 7B–H). The duration of coronavirus disease in patients who were on auxiliary ventilation was significantly associated with the presence of DAD ($p < 0.001$), AFOP ($p = 0.002$; Fig. 7A), heterogeneous hyaline membranes ($p < 0.001$; Fig. 7C), diffuse intraalveolar fibrin organization ($p = 0.021$; Fig. 7D), lymphocytic alveolitis ($p = 0.006$; Fig. 7B), perivascular inflammation ($p < 0.001$; Fig. 7F), pulmonary capillary

congestion ($p < 0.001$; Fig. 7D), single and diffuse alveolar hemorrhages ($p = 0.038$ and $p = 0.036$, respectively; Fig. 7E), focal proliferative interstitial fibroblasts ($p = 0.009$; Fig. 7G), pulmonary embolism ($p = 0.011$; Fig. 7H) comparable to the patients of control group who were also on respiratory support but were not affected by SARS-CoV-2 virus (Fig. 7).

Analysis of morphological changes in the lungs of patients with diagnosed COVID-19 showed significant differences compared with the control group depending on such indicators as Histological diagnosis, Hyaline membranes, Intra-alveolar fibrin organization, Fibrin thrombi, Lymphocytic alveolitis, Perivascular inflammation, Fibrinoid necrosis of vascular walls, Alveolar hemorrhages, Proliferating interstitial fibroblasts, Pulmonary embolism, Pulmonary capillary congestion. Thus, morphological changes such as DAD ($p < 0.001$), diffuse hyaline membranes ($p < 0.001$), focal proliferation interstitial fibroblasts ($p < 0.001$) and others ones were significantly more common in fatal outcomes from COVID-19 (Table 1). All histological and morphological signs correlated with radiology signs (Fig. 3B).

The duration of respiratory support in case of severe COVID-19 patients lasted for approximately ten days before death (Fig. 8). However, some patients could live on auxiliary ventilation for longer periods, up to 78 days (Fig. 8). This was not characteristic of control patients, who were also on respiratory support but were not affected by SARS-CoV-2. Studied morphological changes in the lungs of deceased patients showed strong association with COVID-19. All parameters analyzed allowed distinct clustering of patients with pulmonary disorders and those with COVID-19 (Fig. 9). The majority of variance (49.3%) was explained by the principal component 1 (Fig. 9). Severe COVID-19 in patients on respiratory support was tightly associated with diffuse alveolar damage (attributable risk (AR) = 85.9 (97.0%), $\chi^2 = 54.7$, $p < 0.001$), pulmonary capillary congestion (AR = 83.3 (91.9%), $\chi^2 = 50.7$, $p < 0.001$), and perivascular inflammation (AR = 74.5 (96.1%), $\chi^2 = 40.7$, $p < 0.001$). Odds ratios for the above parameters are shown in the

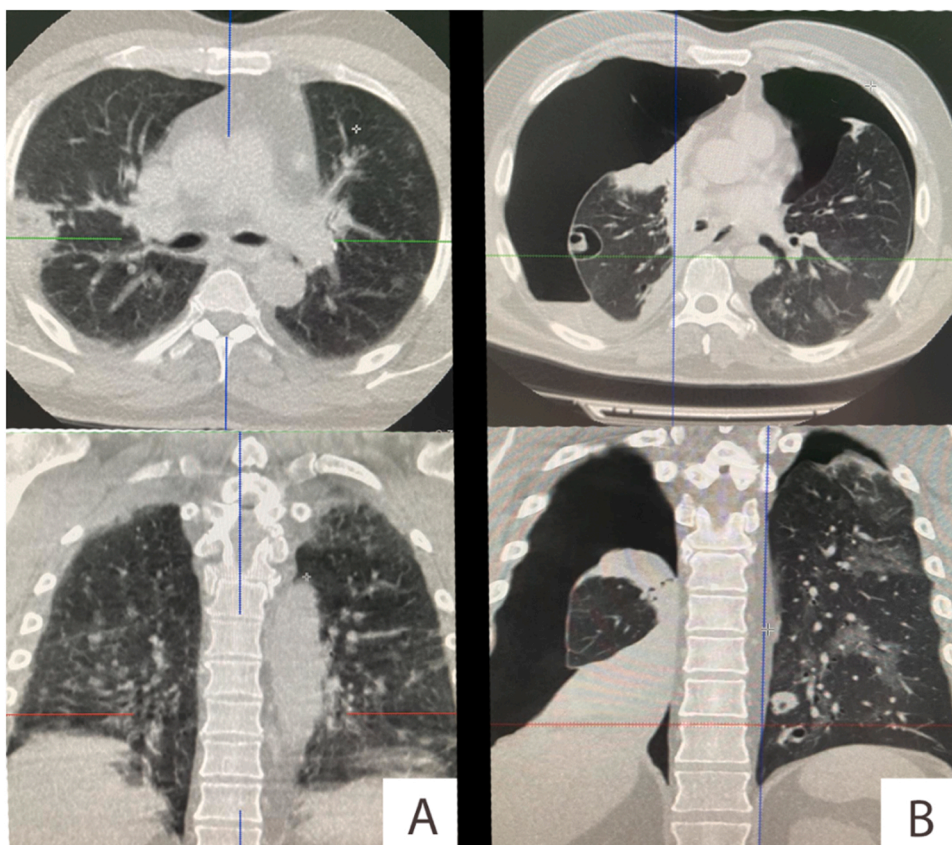


Fig. 5. Vital CT-scans of patient N., 60 years old, with confirmed COVID-19, comorbid hypertension and diabetes mellitus. A. At admission: Axial CT section (upper image) and coronal reconstruction of CT scans (lower image) of the chest: subpleural consolidation of the S4 segment of the right lung diffuse ground glass. B. Significant negative dynamics after 8 days: Axial CT section (upper image) and coronal reconstruction of CT scans (lower image) of the chest: subtotal pneumothorax on the right with areas of consolidation and formation of cavitation, atelectasis, hydrothorax; left pneumothorax locally at the apex with areas of consolidation, ground glass and cavitation. Microbiological analysis of the respiratory tract swabs and tissues did not reveal specific tuberculosis and fungal flora.

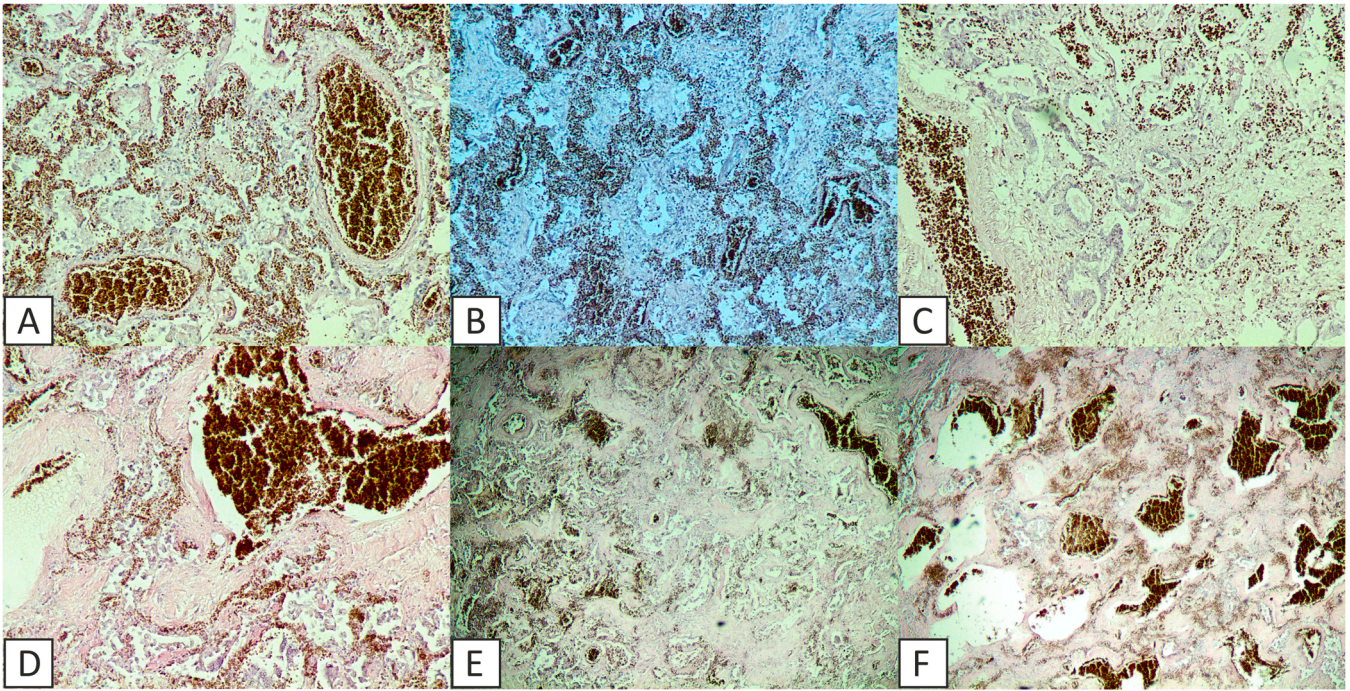


Fig. 6. Histological findings of lungs injured by coronavirus infection (hematoxylin and eosin-stained section; original magnification x 20). A. Exudative stage of diffuse alveolar damage with pulmonary capillary congestion and intravascular erythrocyte aggregation. B. Exudative stage of diffuse alveolar damage. Signs of viral and bacterial pneumonia coexisting: leucocytes deposition in alveoli with thickening of alveolar septa. Microvascular thrombosis. C. Exudative stage of diffuse alveolar damage. Epithelial desquamation of terminal bronchiole, peribronchial edema, pulmonary capillary congestion, intravascular erythrocyte aggregation. D. Exudative stage of diffuse alveolar damage. The destructive-productive vasculitis, perivascular hemorrhage. E. Proliferative stage of diffuse alveolar damage. Squamous epithelial metaplasia, fibrin deposition, alveolar presence of erythrocytes. F. Proliferative stage of diffuse alveolar damage. Fibroblasts proliferation (granulation tissue formation) in the alveoli and perivascular spaces, pulmonary capillary congestion with intravascular erythrocyte aggregation and mural thrombi.

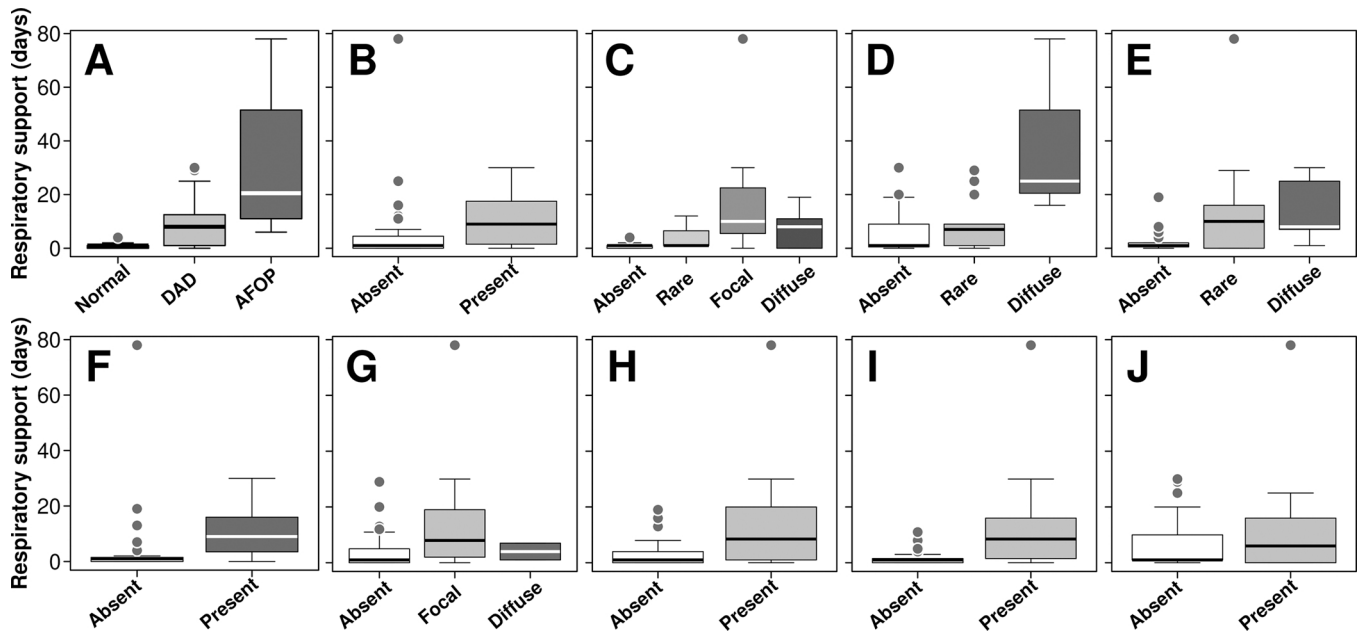


Fig. 7. Respiratory support duration dependence on: A) histological diagnosis – diffuse alveolar damage ($p < 0.001$), acute fibrosing organizing pneumonia ($p = 0.002$); B) lymphocytic alveolitis ($p = 0.006$); C) heterogeneous hyaline membranes ($p < 0.001$); D) diffuse intraalveolar fibrin organization ($p = 0.021$); significant differences in all parameters; E) single and diffuse alveolar hemorrhages ($p = 0.038$ and $p = 0.036$, respectively); F) perivascular inflammation ($p < 0.001$); G) focal proliferation interstitial fibroblasts ($p = 0.009$); H) pulmonary embolism ($p = 0.011$); significant differences in all parameters. I) pulmonary capillary congestion ($p < 0.001$, significant difference), and J) fibrinoid necrosis of vascular walls ($p = 0.610$, no significant difference).

Fig. 10. A weaker association was found for lymphocytic alveolitis (AR = 52.9 (86.4%), $\chi^2 = 18.3$, $p < 0.001$), focal proliferating interstitial fibroblasts (AR = 51.3 (85.5%), $\chi^2 = 16.8$, $p < 0.001$), pulmonary

embolism (AR = 51.8 (79.5%), $\chi^2 = 19.2$, $p < 0.001$), alveolar hemorrhages (AR = 47.9 (77.0%), $\chi^2 = 16.1$, $p < 0.001$), diffuse hyaline membranes (AR = 46.8 (87.5%), $\chi^2 = 10.6$, $p = 0.001$), and fibrinoid

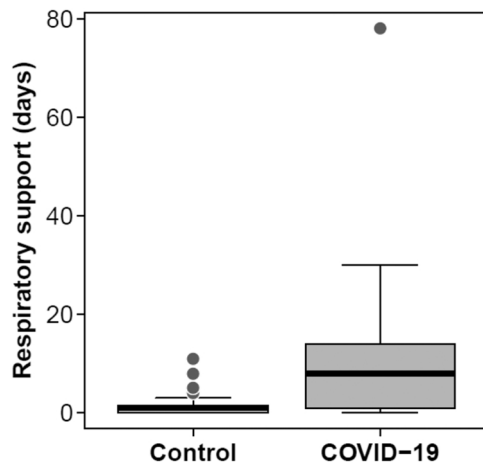


Fig. 8. Duration of respiratory support for the control (lung pneumonia not associated with COVID-19) and study group (COVID-19 patients). The duration of respiratory support of COVID-19 patients was significantly different from the value of this parameter for the control group with $p < 0.001$ according to Mann-Whitney test.

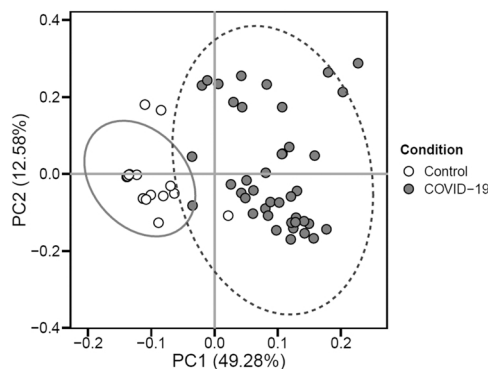


Fig. 9. Principal component analysis for all patients studied using such indicators as “Histological diagnosis”, “Hyaline membranes”, “Intra-alveolar fibrin organization”, “Fibrin thrombi”, “Lymphocytic alveolitis”, “Perivascular inflammation”, “Fibrinoid necrosis of vascular walls”, “Alveolar hemorrhages”, “Proliferating interstitial fibroblasts”, “Pulmonary embolism”, and “Pulmonary capillary congestion”.

wall necrosis (AR = 41.8 (78.0%), $\chi^2 = 9.5$, $p = 0.002$) (Fig. 9). However, lungs of nearly all deceased COVID-19 patients receiving respiratory support had either focal or diffuse hyaline membranes, whereas there was no association for rare hyaline membranes (AR = 29.6 (64.0%), $\chi^2 = 0.9$, $p = 0.332$).

When evaluating the dependence of the probability of death from COVID-19 on respiratory support indicators using ROC analysis, the following curves were obtained (Fig. 11). The resulting patterns were statistically significant ($p < 0.001$). The threshold value of the indicator “Respiratory support (days)” at the cut-off point, which corresponded to the highest value of the Youden index, was 5000. Lethal outcome due to COVID-19 was predicted if the value of the indicator Respiratory support is higher than or equal to this value. The sensitivity and specificity of the model were 68.3% and 87.5%, respectively. The threshold value of the indicator Face mask respiratory support at the cut-off point, which corresponded to the highest value of the Youden index, was 1000. Lethal outcome due to COVID-19 was predicted if the value of the indicator Face mask respiratory support was higher than or equal to this value. The sensitivity and specificity of the model were 78.0% and 71.9%, respectively.

4. Discussion

Previous studies aimed to determine predictors of mortality from COVID-19, which also included cohort autopsies, indicate the importance of hematologic (neutrophil, lymphocyte counts and their ratio), inflammatory (C-reactive protein, erythrocyte sedimentation rate, interleukin-6), biochemical (D-dimer, troponins, liver samples) indicators and coagulograms, as well as pathophysiological processes of systemic and metabolic changes as determinants of the unfavorable prognosis of COVID-19. We also suggest that with such multifactorial changes and rapid progression of the disease, the use of artificial ventilation is limited in patients with COVID-19, and sometimes even causes additional lung damage [10]. Moreover, respiratory support is one of the most important aspects in the treatment of patients with severe coronavirus infection who have developed hypoxemia and is life-saving for most patients. Statistically significant changes in patients with coronavirus infection emphasize the actual damaging target effects of SARS-CoV-2 virus on lung tissue, as the use of similar respiratory support in patients without coronavirus disease was not manifested by the above morphological postmortem examination. It is known that a significant amount of virus detected in the respiratory tract exacerbates diffuse alveolar damage and airway obstruction associated with impaired ventilation, which supports the cytotoxic effect of SARS-CoV-2 and causes respiratory failure, and a decrease in viral RNA is characteristic of the course of the disease with morphological manifestations of reduced lung epithelial cell proliferation and the formation of severe pulmonary fibrosis [11]. Of interest for comparison are the data of V. Skoryk et al., according to which scientists have shown the effect of long-term respiratory support on accelerating the development of irreversible processes in the lungs, namely the development of pneumofibrosis and complications due to the accession of ventilation-associated pneumonia [12] barotrauma in patients with COVID-19 due to the coexistence of severely affected areas of the lungs adjacent to relatively unaffected areas. Affected areas with atelectasis cannot or are very difficult to straighten by selecting ventilation parameters or increasing the pressure at the end of exhalation. At the same time, the unaffected areas remain extremely sensitive and reactive, and therefore at risk of overstretching due to the supply of higher pressure [7]. Therefore, in patients with severe respiratory distress syndrome, the strategy of preventing atelectasis injury by increasing blood pressure may be detrimental. Therefore, mechanical ventilation should also be aimed at preventing damage caused by ventilators while protecting intact lung tissue [13].

Post-mortem diagnosis, especially for newly studied new diseases, plays a critical role in understanding the mechanism of pathogenesis and the prevalence of lesions, which can often be invisible in life. According to autopsy studies E.E. Tejerina et al., Conducted in the pre-COVID-19 period, in 17.7% of cases missed the diagnosis, in 8.4% had a discrepancy in the diagnosis of class I, in 9.3% - a discrepancy of class II [14]. Complete autopsy with SARS-CoV-2 allows to obtain samples for PCR to determine the localization of the virus in inaccessible locations in life, to compare the radiological picture of lung involving with morphological one, to compare histological findings in new coronavirus infection with pathomorphological results of respiratory syndromes of previous viral pandemic, to supplement the database of own practical and interesting cases for presentation to the scientific community.

Analyzing the results of morphological study of the lungs in our study and comparing it with data obtained by other scientists, the presence of different stages of DAD, endothelitis, capillary congestion is noteworthy, which determines the predominant lethal outcomes caused by respiratory failure [15–19]. In all patients from the study who died of coronavirus infection, the main comorbid diseases were arterial hypertension, diabetes mellitus, heart failure, coronary artery disease, obesity, chronic renal failure, malignancy, which was consistent with the results obtained by other scientists [20–24].

If we compare the histopathological findings in SARS-CoV-2 and the

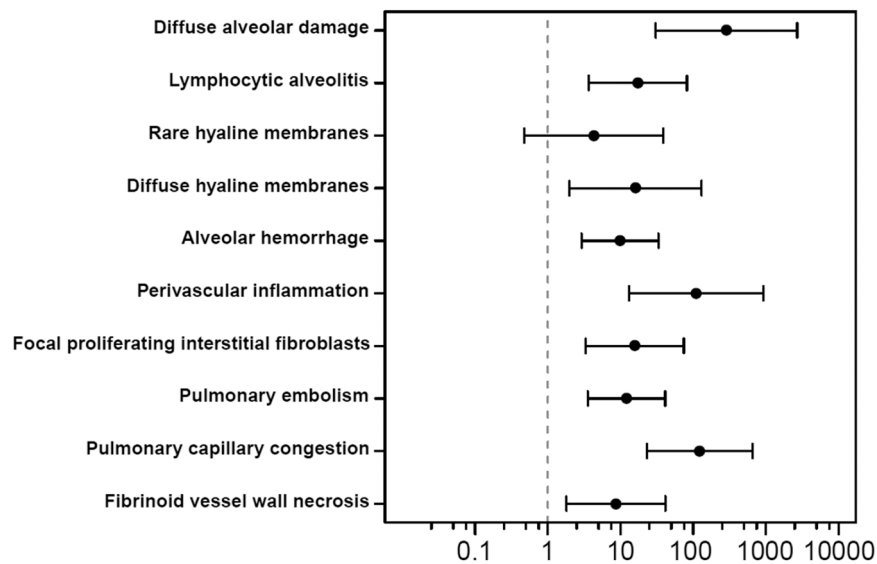


Fig. 10. Association of each of measured parameters with COVID-19 and non-COVID-19 mortality. Dots represent odds ratios with 0.95 confidence intervals (error bars).

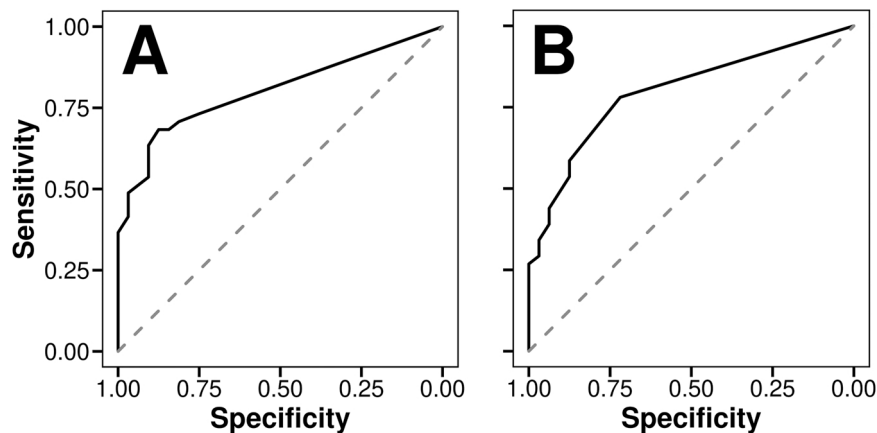


Fig. 11. A. ROC-curve characterizing the dependence of lethal outcomes on the total respiratory support duration. The sensitivity and specificity were 68.3% and 87.5%, respectively. B. ROC-curve characterizing the dependence of lethal outcomes on the duration of face mask respiratory support. The sensitivity and specificity were 78.0% and 71.9%, accordingly.

pandemic Influenza A (H1N1), the latter was also characterized by diffuse alveolar damage at different stages, acute, necrotizing bronchopneumonia prominent peripheral pulmonary vascular thrombosis and hemophagocytosis [25]. A similar histopathological picture is described for Severe acute respiratory syndrome associated coronavirus (SARS-CoV), a pandemic that lasted from 2002 to 2003, where the authors emphasize the dependence of the stages of diffuse alveolar damage on the duration of the disease [26]. Additionally, in addition to DAD, another group of scientists has identified signs of bronchial epithelial exposure, eyelash loss, and squamous metaplasia [27]. For Middle East respiratory syndrome - coronavirus (MERS-CoV), which was first detected in 2012, the main histopathological findings in the respiratory tract were severe acute haemorrhagic pneumonia, exudative DAD, type II pneumocyte hyperplasia, single syncytial cells, and interstitial septal lymphoid [16,28]. As can be seen, DAD is common for respiratory syndromes caused by the coronavirus family and the H1N1 influenza virus. It is also impossible to reduce the prevalence of other histological findings for previous types of respiratory syndromes, because autopsy samples for them were not equivalent in number to SARS-CoV-2. It should also be noted that the absence of DAD does not preclude the presence of COVID-19 and in the absence of lifelong testing and the

presence of suspected coronavirus infection, PCR of autopsy material should be performed [29]. Also, the various stages of DAD, from exudative to acute fibrinous and organizing pneumonia (the latter some also refer to as an unusual histological pattern rather than the final stage of DAD) present, are explained by different lung compliance in the early and late stages of the disease [30,31]. In fact, the latter cannot always be established accurately, as some patients seek help too late and the duration of the disease is unknown. Concomitant bacterial infection with lung tissue damage may also play a key role in the stages of DAD [32].

It should also be borne in mind that the use of mechanical lung ventilation, according to a prospective cohort study, is a risk factor for pulmonary embolism along with such independent factors as overweight, male gender, prolonged lying down and the presence of malignancies that are similar predictors of severe COVID-19, so the occurrence of thromboembolism in patients with SARS-CoV-2, whose respiration is maintained by mechanical ventilation, may be poly-etiological in nature [33]. According to A.C. Borczuk's use of viral diagnostic methods based on RNA in-situ hybridization and tissue-based PCR allows the recognition of primary viral lung damage from ventilator-associated pneumonia [34]. Also, some morphological signs

are found both in the study group and in several patients in the control group, namely: pulmonary embolism, pulmonary capillary congestion, rare fibrin thrombi, lymphocytic alveolitis, rare alveolar hemorrhages, rare proliferating interstitial fibroblasts. It should be noted that the patients selected for the control group were also on oxygen support (to consider the influence of mechanical ventilation on both groups). Such morphological changes in patients of the control group may correspond to ventilation-associated injury, as well as the pathogenesis of the development of multiple organ failure in the agonal status of patients who were in a coma of non-respiratory origin [35–38].

Thus, the variability of the histological picture is the cumulative result in each case of the duration and severity of the disease, immune reactivity, viral load, duration and choice of therapy and respiratory support, comorbid diseases. Therefore, the complexity and limitation of the study is to identify the cause of the histological pattern as the autopsy of patients with particularly dangerous infections, including COVID-19, does not include previous biopsy results that could clearly correlate with changes in clinical or radiological picture. Changes that may occur in different tissues from death to autopsy should also be considered and require further study of such effects on enzyme-linked immunosorbent assays and molecular parameters.

5. Conclusions

For patients with COVID-19 on long-term respiratory support with radiological signs of ground glass opacity and lung consolidation, the characteristic postmortem morphological features were diffuse alveolar lung damage at various stages of development, pulmonary capillary congestion, fibrin clots and perivascular inflammation.

Institutional Review Board Statement

The study was conducted according to the guidelines of the Declaration of Helsinki and approved by the Ethics Committee of Ivano-Frankivsk National Medical University (Protocol № 116/20 of 07.10.2020).

Informed Consent Statement

Informed consent was obtained from legally authorized person of deceased patients involved in the study.

Funding

This research was funded by the National Research Foundation of Ukraine (project registration number 2020.01/0157).

CRedit authorship contribution statement

Conceptualization, V.V., A.K., D.G., O.L.; Methodology, T.L.; Software, A.K.; Validation, R.F., V.M.V., M.M.; Formal Analysis, A.K., I.Y.; Investigation, V.V.; Resources, M.M., V.B.; Data Curation, T.L.; Writing – Original Draft Preparation, V.V., A.K., D.G., P.P.; Writing – Review & Editing, O.L.; Visualization, V.V.; Supervision, O.L.; Project Administration, R.F.; Funding Acquisition, D.G., I.Y., O.L. All authors have read and agreed to the published version of the manuscript.

Declaration of Competing Interest

The authors declare that they have no known competing financial interests or personal relationships that could have appeared to influence the work reported in this paper.

Data Availability

Not applicable.

Appendix A. Supporting information

Supplementary data associated with this article can be found in the online version at [doi:10.1016/j.prp.2023.154471](https://doi.org/10.1016/j.prp.2023.154471).

References

- [1] World Health Organization. WHO Coronavirus (COVID-19) Dashboard. 2023. Available online: <https://covid19.who.int/> (Accessed on 17 April 2023).
- [2] K. Yuki, M. Fujiogi, S. Koutsogiannaki, COVID-19 pathophysiology: a review, *Clin. Immunol.* 215 (2020), 108427, <https://doi.org/10.1016/j.clim.2020.108427>.
- [3] National Institutes of Health. Treatment Guidelines Panel. Coronavirus Disease 2019 (COVID-19). Nih 2021, 2019. Available online: <https://www.covid19treatmentguidelines.nih.gov/>.
- [4] G. Allali, C. Marti, O. Grosgrin, C. Morélot-Panzini, T. Similowski, D. Adler, Dyspnea: the vanished warning symptom of COVID-19 pneumonia, *J. Med Virol.* 92 (2020) 2272–2273, <https://doi.org/10.1002/jmv.26172>.
- [5] T. Montrieff, M. Ramzy, B. Long, M. Gottlieb, D. Hercz, COVID-19 respiratory support in the emergency department setting, *Am. J. Emerg. Med.* 38 (2020) 2160–2168, <https://doi.org/10.1016/j.ajem.2020.08.001>.
- [6] T. Bradley, H. Maioli, R. Johnston, I. Chaudhry, L. Fink, H. Xu, et al., Histopathology and ultrastructural findings of fatal COVID-19 infections in Washington state: a case series, *Lancet* 396 (2020) 320–332, [https://doi.org/10.1016/S0140-6736\(20\)31305-2](https://doi.org/10.1016/S0140-6736(20)31305-2).
- [7] M. Dondorp, M. Hayat, D. Aryal, A. Beane, J. Schultz, Respiratory support in COVID-19 patients, with a focus on resource-limited settings, *Am. J. Trop. Med Hyg.* 102 (2020) 1191–1197, <https://doi.org/10.4269/ajtmh.20-0283>.
- [8] Matskevych V., Vasylyk V., Kamyshnyi A., Lenchuk T., Lushchak O., Yurkevych I., Fishchuk R., inventors, assignee. Method of sectional biological material samples collecting at diffuse alveolar damage of lungs of infectious origin [Sposib zaboru sektiynoho biolohichnoho material pry dyfuznomu poshkodzhenni lehen infektsiynoho henezuj]. Ukraine patent UA 146810. 2021.
- [9] Centers for Disease Control and Prevention. Available online: <https://www.cdc.gov/coronavirus/2019-ncov/hcp/guidance-postmortem-specimens.html> (Accessed on 17 October 2022).
- [10] G. Ponti, M. Maccaferri, C. Ruini, A. Tomasi, T. Ozben, Biomarkers associated with COVID-19 disease progression (<https://doi.org/10.1080/10408363.2020.1770685>), *Crit. Rev. Clin. Lab Sci.* 57 (2020) 389–399, <https://doi.org/10.1080/10408363.2020.1770685>.
- [11] H. Yao, T. Luo, Y. Shi, C. He, R. Tang, P. Zhang, et al., A cohort autopsy study defines COVID-19 systemic pathogenesis, *Cell Res* 31 (2021) 836–846, <https://doi.org/10.1038/s41422-021-00523-8>.
- [12] V. Skoryk, V. Korsunov, T. Bocharova, P. Nartov, M. Valentina, Clinical and morphological comparison of respiratory failure in patients with COVID-19 who died under different options of respiratory support, *Sci. Med Sci.* 4 (2021) 4–12, <https://doi.org/10.15587/2519-4798.2021.238093>.
- [13] M. Constantin, M. Jabaudon, Y. Lefrant, S. Jaber, P. Quenot, O. Langeron, et al., Personalised mechanical ventilation tailored to lung morphology versus low positive end-expiratory pressure for patients with acute respiratory distress syndrome in France (the LIVE Study): a multicentre, single-blind, randomised controlled trial, *Lancet Respir. Med* 7 (2019) 870–880, [https://doi.org/10.1016/S2213-2600\(19\)30138-9](https://doi.org/10.1016/S2213-2600(19)30138-9).
- [14] E.E. Tejerina, R. Padilla, E. Abril, F. Frutos-Vivar, A. Ballen, J.M. Rodríguez-Barbero, et al., Autopsy-detected diagnostic errors over time in the intensive care unit, *Hum. Pathol.* 76 (2018) 85–90, <https://doi.org/10.1016/j.humpath.2018.02.025>.
- [15] F. Lax, K. Skok, P. Zechner, H. Kessler, N. Kaufmann, C. Koelblinger, et al., Pulmonary arterial thrombosis in COVID-19 with fatal outcome: results from a prospective, single-center, clinicopathologic case series, *Ann. Intern Med* 173 (2020) 350–361, <https://doi.org/10.7326/M20-2566>.
- [16] T. Menter, D. Haslbauer, R. Nienhold, S. Savic, H. Hopfer, N. Deigendesch, et al., Postmortem examination of COVID-19 patients reveals diffuse alveolar damage with severe capillary congestion and variegated findings in lungs and other organs suggesting vascular dysfunction, *Histopathology* 77 (2020) 198–209, <https://doi.org/10.1111/his.14134>.
- [17] T. Schaller, K. Hirschbühl, K. Burkhardt, G. Braun, M. Trepel, B. Märkl, et al., Postmortem examination of patients with COVID-19, *JAMA* 323 (2020) 2518–2520, <https://doi.org/10.1001/jama.2020.8907>.
- [18] C. Edler, A.S. Schröder, M. Aepfelbacher, A. Fitzek, A. Heinemann, F. Heinrich, et al., Dying with SARS-CoV-2 infection—an autopsy study of the first consecutive 80 cases in Hamburg, Germany, *Int. J. Leg. Med* 47 (2020), 101769, <https://doi.org/10.1007/s00414-020-02336-7>.
- [19] D. Wichmann, P. Sperhake, M. Lütgehetmann, S. Steurer, C. Edler, A. Heinemann, et al., Autopsy findings and venous thromboembolism in patients with COVID-19: a prospective cohort study, *Ann. Intern Med* 173 (2020) 268–277, <https://doi.org/10.7326/M20-2003>.
- [20] K. Evert, T. Dienemann, C. Brochhausen, D. Lunz, M. Lubnow, M. Ritzka, et al., Autopsy findings after long-term treatment of COVID-19 patients with microbiological correlation, *Virchows Arch.* 479 (2021) 97–108, <https://doi.org/10.1007/s00428-020-03014-0>.
- [21] C. Magro, J. Mulvey, D. Berlin, G. Nuovo, S. Salvatore, J. Harp, et al., Complement associated microvascular injury and thrombosis in the pathogenesis of severe COVID-19 infection: a report of five cases, *Transl. Res* 220 (2020) 1–13, <https://doi.org/10.1016/j.trsl.2020.04.007>.

- [22] Z. Varga, J. Flammer, P. Steiger, M. Haberecker, R. Andermatt, S. Zinkernagel, et al., Endothelial cell infection and endotheliitis in COVID-19, *Lancet* 395 (2020) 1417–1418, [https://doi.org/10.1016/S0140-6736\(20\)30937-5](https://doi.org/10.1016/S0140-6736(20)30937-5).
- [23] M. Haberecker, I. Schwarz, P. Steiger, K. Frontzek, F. Scholkmann, X. Zeng, et al., Autopsy-based pulmonary and vascular pathology: pulmonary endotheliitis and multi-organ involvement in COVID-19 associated deaths, *Respiration* 101 (2022) 155–165, <https://doi.org/10.1159/000518914>.
- [24] C. Borczuk, P. Salvatore, V. Seshan, S. Patel, B. Bussel, M. Mostyka, et al., COVID-19 pulmonary pathology: a multi-institutional autopsy cohort from Italy and New York City, *Mod. Pathol.* 33 (2020) 2156–2168, <https://doi.org/10.1038/s41379-020-00661-1>.
- [25] W. Harms, A. Schmidt, B. Smith, W. Newton, A. Pletneva, L. Walters, et al., Autopsy findings in eight patients with fatal H1N1 influenza, *Am. J. Clin. Pathol.* 134 (2010) 27–35, <https://doi.org/10.1309/AJCP35KOZSAVNQZW>.
- [26] J. Franks, Y. Chong, P. Chui, R. Galvin, M. Lourens, H. Reid, et al., Lung pathology of severe acute respiratory syndrome (SARS): a study of 8 autopsy cases from Singapore, *Hum. Pathol.* 34 (2003) 743–748, [https://doi.org/10.1016/s0046-8177\(03\)00367-8](https://doi.org/10.1016/s0046-8177(03)00367-8).
- [27] M. Nicholls, M. Poon, C. Lee, F. Ng, T. Lai, Y. Leung, et al., Lung pathology of fatal severe acute respiratory syndrome, *Lancet* 361 (2003) 1773–1778, [https://doi.org/10.1016/s0140-6736\(03\)13413-7](https://doi.org/10.1016/s0140-6736(03)13413-7).
- [28] O. Alsaad, H. Hajeer, M. Al Balwi, M. Al Moaiqel, N. Al Oudah, A. Al Ajlan, et al., Histopathology of middle east respiratory syndrome coronavirus (MERS-CoV) infection – clinicopathological and ultrastructural study (<https://doi.org/>), *Histopathology* 72 (2018) 516–524, <https://doi.org/10.1111/his.13379>.
- [29] Sekhawat V., Green A., Mahadeva U. COVID-19 Autopsies: Conclusions from International Studies. *Diagnostic Histopathol.* 27:103–107. <https://doi.org/http://doi.org/10.1016/j.mpdhp.2020.11.008>.
- [30] L. Gattinoni, D. Chiumello, S. Rossi, COVID-19 pneumonia: ARDS or not? *Crit. Care* 24 (2020) 154, <https://doi.org/10.1186/s13054-020-02880-z>.
- [31] C. Santos, C. Oliveira, P. Serra, P. Baptista, E. Sousa, P. Casanova, et al., Pathophysiology of acute fibrinous and organizing pneumonia – clinical and morphological spectra, *Pathophysiology* 26 (2019) 213–217, <https://doi.org/10.1016/j.pathophys.2019.04.001>.
- [32] M. Rimmelink, R. De Mendonça, N. D’Haene, S. De Clercq, C. Verocq, L. Lebrun, et al., Unspecific post-mortem findings despite multiorgan viral spread in COVID-19 patients, *Crit. Care* 24 (2020) 495, <https://doi.org/10.1186/s13054-020-03218-5>.
- [33] C. Minet, M. Lugosi, Y. Savoye, C. Menez, S. Ruckly, A. Bonadona, et al., Pulmonary embolism in mechanically ventilated patients requiring computed tomography: prevalence, risk factors, and outcome, *Crit. Care Med* 40 (2012) 3202–3208, <https://doi.org/10.1097/CCM.0b013e318265e461>.
- [34] C. Borczuk, Pulmonary pathology of COVID-19: a review of autopsy studies (<https://doi.org/>), *Curr. Opin. Pulm. Med* 27 (2021) 184–192, <https://doi.org/10.1097/MCP.0000000000000761>.
- [35] S.W. Aesif, A.C. Bribresco, R. Yadav, S.L. Nugent, D. Zubkus, C.D. Tan, et al., Pulmonary pathology of COVID-19 following 8 weeks to 4 months of severe disease: a report of three cases, including one with bilateral lung transplantation, <https://doi.org/10.1093/ajcp/aqaa264>, *Am. J. Clin. Pathol.* 155 (4) (2021) 506–514, <https://doi.org/10.1093/ajcp/aqaa264>.
- [36] Duarte-Neto, Amaro nunes and dolhnikoff, marisa. what remains in the pulmonary tissue after acute COVID-19? ([online]), *J. Bras. De. Pneumol. v. 48* (n. 03) (2022), e20220209, <https://doi.org/10.36416/1806-3756/e20220209>.
- [37] M. Suárez-Pinilla, I. Fernández-Vega, An acute metabolic insult highly increased postmortem cerebellar autolysis: an autopsy case, *Clin. Neuropathol.* 34 (3) (2015) 166–168, <https://doi.org/10.5414/NP300809>.
- [38] M.M. Adeva, G. Souto, C. Donapetry, M. Portals, A. Rodriguez, D. Lamas, Brain edema in diseases of different etiology, *Neurochem Int* 61 (2012) 166–174, <https://doi.org/10.1016/j.neuint.2012.05.007>.